

UC Riverside

UC Riverside Electronic Theses and Dissertations

Title

An Investigation of Natural Convection in a Horizontal Concentric Annuli With Different Inner Shapes

Permalink

<https://escholarship.org/uc/item/2vt3w60s>

Author

Yuan, Xing

Publication Date

2014

Peer reviewed|Thesis/dissertation

UNIVERSITY OF CALIFORNIA
RIVERSIDE

An Investigation of Natural Convection in a Horizontal Concentric Annuli With Different
Inner Shapes

A Thesis submitted in partial satisfaction
of the requirements for the degree of

Master of Science

in

Mechanical Engineering

by

Xing Yuan

August 2014

Thesis Committee:

Dr. Kambiz Vafai, Chairperson
Dr. Marko Princevac
Dr. Guanshui Xu

Copyright by
Xing Yuan
2014

The Thesis of Xing Yuan is approved:

Committee Chairperson

University of California, Riverside

ACKNOWLEDGEMENTS

I would like to thank my advisor Prof, Kambiz Vafai, who helped me a lot in my life and study here in UCR. I also want to give my thanks to Prof. Marko Princevac and Prof. Guanshui Xu who enriched my work greatly using their knowledge.

I want to express my gratitude to my friends Yuxiang Qin and Mian Zhou. It was them who drive me back every single time when I study late in the lab even in the midnight. They gave me so many helps when I was in difficult situation.

I want to thank my friends Shujuan Wang, Xi Chen, Marcello Lasiello and Keyong Wang who gave me many suggestions on my research.

I want to thank my family, it is them who always stand beside me and support my way to my dream

I want to thank my girlfriend specially, it was her who gave me encouragement when I was in upset. She is the shiniest star in my sky.

DEDICATION

This work is dedicated to my parents Baoqing Yuan and Guiying Wang, and my girlfriend Yaqiong Li. I love them forever.

ABSTRACT OF THE THESIS

An Investigation of Natural Convection in a Horizontal Concentric Annuli With Different Inner Shapes

by

Xing Yuan

Master of Science, Graduate Program in Mechanical Engineering
University of California, Riverside, August 2014
Dr. Kambiz Vafai, Chairperson

An investigation of free convection in a horizontal concentric annuli with different inner shapes where the inner and outer surfaces are kept at a constant temperature is presented. The simulation is categorized into four groups based on the shape of the inner entity which can be either cylindrical, elliptical, square or triangular. Flow and thermal fields are exhibited by means of streamlines and isotherms. Overall heat transfer correlations incorporating thermal radiation are established and presented in terms of the Nusselt numbers. It is observed that the surface radiation and existence of the corners and larger top space can enhance the heat transfer rate. As the reference temperature and Rayleigh number increases, surface radiation plays a more prominent role in the overall heat transfer performance.

Keywords: Natural convection, inner shapes, radiation, annuli

Table of Content

| | |
|--|------|
| Acknowledgements..... | iv |
| Dedication..... | v |
| Abstract..... | vi |
| Table of Contents..... | vii |
| List of Tables..... | viii |
| List of Figures..... | ix |
| Nomenclature..... | xi |
| Chapter 1 Introduction..... | 1 |
| Chapter 2 Formulation..... | 6 |
| 2.1 Model Description..... | 6 |
| 2.2 Governing Equations..... | 7 |
| 2.3 Radiation Exchange..... | 9 |
| Chapter 3 Validation..... | 10 |
| Chapter 4 Results and Discussions..... | 11 |
| 4.1 Streamlines and Isotherms..... | 11 |
| 4.2 Local Nusselt Number..... | 12 |
| 4.3 Heat Transfer Correlations..... | 14 |
| Chapter 5 Conclusions..... | 16 |
| References..... | 33 |

List of Tables

| | |
|--|----|
| Table 1 Reference fluid properties..... | 17 |
| Table 2 Grid independence test performed at $T_{ref} = 573K$, $Pr = 0.674$ and $Ra = 10^6$ | 18 |
| Table 3 Comparison of the average heat transfer results for a cylindrical annulus with Kuehn and Goldstein [22]..... | 19 |
| Table 4 Comparison of the average heat transfer results for a square inner configuration with Chang et al. [23]..... | 20 |
| Table 5 Total average Nusselt number correlations at the inner surface for different inner shapes | 21 |

List of Figures

| | |
|--|----|
| Figure. 1 Concentric annuli with different inner shapes. | 22 |
| Figure. 2 Comparison of the present results with Kuehn and Goldstein [22] at (a) Local equivalent conductivity along the inner and outer surface (b) Dimensionless radial temperature | 23 |
| Figure. 3 Streamlines in an annulus with different inner shapes: Circular, Elliptical, Square and Triangular at different Rayleigh numbers. | 24 |
| Figure. 4 Isotherms in an annulus with different inner shapes: Circular, Elliptical, Square and Triangular at different Rayleigh numbers | 25 |
| Figure. 5 Comparison of the local Nusselt number between pure convection and convection and radiation for a cylindrical annulus..... | 26 |
| Figure. 6 Comparison of the local Nusselt number between pure convection and convection and radiation for a elliptical annulus..... | 27 |
| Figure. 7 Comparison of the local Nusselt number between pure convection and convection and radiation for a square annulus | 28 |
| Figure. 8 Comparison of the local Nusselt number between pure convection and convection and radiation for a triangular annulus | 29 |
| Figure. 9 Effect of the Rayleigh number on the Nusselt number distribution for Cylindrical inner surface (a) Inner wall, (b) Outer wall. Elliptical inner surface (c) Inner wall, (d) Outer wall | 30 |

Figure. 10 Effect of the Rayleigh number on the Nusselt number distribution for Square inner surface (a) Inner wall, (b) Outer wall. Triangular inner surface (c) Inner wall, (d) Outer wall 31

Figure. 11 Comparison of the Nusselt number distributions for different inner shapes at $Ra = 5 \times 10^4$, (a) and (b): $T_{ref} = 573K$ (c) and (d): $T_{ref} = 1273K$ 32

Nomenclature

| | | | |
|-----------------|--|---------------------|--|
| A | Surface area for heat transfer | α | Thermal diffusivity, m^2 / s |
| D | Diameter | β | Thermal expansion coefficient, $1 / K$ |
| g | Gravitational acceleration, m / s^2 | ε | Average emissivity |
| Gr | Grashof number | μ | Viscosity, $kg / (m \cdot s)$ |
| k | Thermal conductivity, $W / (m \cdot K)$ | ρ | Density, kg / m^3 |
| K_{eq} | Equivalent conductivity | θ | Angular coordinate |
| L | Equivalent annulus gap width | | |
| $\frac{Nu}{Nu}$ | Local and average Nusselt number | Subscripts | |
| P | Pressure, Pa | i | Inner |
| Pr | Prandtl number | o | Outer |
| q | Local heat flux, W / m^2 | ref | Reference quantities |
| Q | Overall heat flux, W / m | c | Convection |
| Ra | Raleigh number, $= \frac{g\beta(T_i - T_o)L^3\rho}{\alpha\mu}$ | r | Radiation |
| T | Temperature, K | | |
| T_{ref} | Reference temperature, $= (T_i + T_o) / 2$, K | Superscripts | |
| u, v | Velocities in the x- and y- directions | $*$ | Dimensionless quantities |

Chapter 1

Introduction

Natural convection heat transfer within an annulus has been the subject of interest for decades. Natural convection in a finite space is important for many applications, including design of electronic equipment cooling systems, nuclear reactor waste transport and storage, solar collectors and thermal storage systems and thermal management of aviation.

Natural convection in an enclosure can vary quite substantially due to the geometry of the enclosure. There are a significant number of reported experimental, analytical and numerical studies on natural convection in an annulus with different kinds of boundary conditions in the literature. These articles address the effects of Rayleigh number, Prandtl number, the influence of different media, the influence of different inner and outer boundary shapes, the ratio of the gap width to inner characteristic diameter and the effect of inclination angle and eccentricity [1-17].

Angeli et al. [1] displayed the evolution of the flow regimes and temperature patterns within a horizontal annulus with increasing values of the Rayleigh number. For very low Rayleigh number (Ra) values, the regime is pseudo-diffusive, and the heat transfer process is conduction-dominated. Such a regime persists as long as the annular gap L and/or the temperature difference between the inner and outer walls are sufficiently small. Numerical calculations have also been performed by Ho et al. [2] for an annulus with a radius ratio fixed at 2.6 to investigate the effect of variations in Ra and Pr on the fluid flow pattern and heat transfer rate. Their work was based on a steady laminar two dimensional natural

convection in a cylindrical annuli with constant heat flux on the inner wall and isothermal temperature on the outer wall. They showed that the influence of the Prandtl number is quite weak and that the heat and fluid flows are primarily dependent on the Ra number and the eccentricity of the annulus. In this work, we set the Prandtl number, Pr at a specified value based on the reference temperature T_{ref} , and focus on investigating the influence of Ra and Radiation effects.

Shu et al. [3] clarified the effects of the eccentricity of the inner cylinder on the local and overall heat transfer coefficients. It was found that global re-circulation, flow separation and the space between the two cylinders have significant effects on the plume inclination and that the overall heat transfer improves with eccentricity except in the middle region where the overall Nusselt number remains at the same level as that for the concentric case.

The effects of thermal radiation on natural convection has been investigated by Han and Baek [4] and Shaija and Narasimham [5]. The working medium was assumed to be homogeneous and gray. It was found that the radiation effect causes the temperature distribution to be more uniform which could reduce the convective heat transfer while the average heat transfer rate was enhanced due to the radiation effect. Tan and Howell [6] discussed the influences of radiation-conduction parameter, Rayleigh number and other parameters on flow and temperature distributions and heat transfer in a two dimensional participating square medium.

The effect of radiation on natural convection is typically more prominent than the forced convection case due to the coupling between the temperature and flow fields in natural

convection. Akiyama and Chong [7] investigated a model for prediction of the influence of gray surface radiation on natural convection in a square enclosure. It was found that the Nusselt number for natural convection with surface radiation can be expressed as a function of Ra and emissivity, ε as $Nu = 0.529Ra^{0.3065}\varepsilon^{0.3497}$.

There are several articles on natural convection within annuli with different shape boundaries. Sambamurthy et al. [8] performed a numerical study of two-dimensional conjugate natural convection in a horizontal cylindrical annulus between an inner heat generating solid square element and an outer isothermal circular boundary. Correlations were developed for estimating various quantities of interest for different configurations, and thermal conductivity and aspect ratios.

Xu et al. [9] have investigated laminar natural convective heat transfer for air within a horizontal annulus between a heated triangular element and its circular cylindrical outer enclosure. They displayed the influence of Rayleigh number, radius ratio and inclination angle on the stream function and the local and average Nusselt numbers. It was found that the inclination angle of the inner triangular cylinder has a negligible effect on the average Nusselt number at a constant radius ratio. Xu et al. [10] also looked into an annulus composed of a horizontal cylinder inside a concentric triangular enclosure. They found that, the overall heat transfer rate was independent of the inclination angle and the geometrical cross section even though the flow patterns was substantially modified.

Yu et al. [11] explored the Prandtl number effect on laminar convection from a horizontal triangular element to its concentric cylindrical enclosure. They had shown that the

temperature distribution was almost independent of the Prandtl number, Pr when $Pr \geq 0.7$, especially at lower Ra numbers.

Boyd [12] experimentally studied the steady natural convective heat transfer across an annulus with an inner hexagonal cylinder and an outer concentric circular cylinder. Their model was based on a liquid metal fast breeder reactor spent fuel subassembly inside a shipping container. The correlation for the mean Nusselt number at the surface of the inner cylinder was expressed as $\overline{Nu} = 0.794Ra_R^{0.25}$. They showed that the existence of the inner hexagonal element corners as compared to an inner circular cylinder, enhances the mean heat transfer.

Shu et al. [13] numerically studied the natural convective heat transfer in a horizontal eccentric annulus between a square outer enclosure and a heated circular inner cylinder. It was found that the flow separation at the top space between the square outer enclosure and the circular inner cylinder has a significant effect on the plume inclination. Natural convection between concentric heated horizontal circular cylinder and cooled square enclosure has been numerically studied by Moukalled [14]. The local Nusselt number along the inner wall displayed a flat trend while the Nusselt number along the outer surface has a peak near the top, which was different from that in a cylindrical annulus under the same condition. Free convection in a vertical or inclined annulus has also been investigated by many authors such as Keyhani et al. [15] and Hamad [16].

The transient natural convection between two horizontal isothermal cylinders could be found in Tsui and Tremblay [17]. In most application cases, the transition time from the

transient state to the steady state is found to be very small in comparison with typical operational times. Vafai and Etefagh [18] explored a transient three-dimensional buoyancy driven flow inside a horizontal annulus. They found that the temperature distribution remains unchanged in the central region provided that the annulus length to outer radius ratio is larger than a critical value.

Aside from the steady flow, Desai and Vafai [19] simulated the turbulent flow region in a horizontal cylindrical annulus. They found that there exists a core region over a substantial length of the cavity which can be simplified into a two-dimensional model. Vafai and Desai [20] also compared the finite-element and finite difference methods in simulating the natural convection in annular cavities. It was shown that the finite element method can produce results which can match the refined finite difference results.

There has been a significant number of investigations related to natural convection in an annulus. However, the effect of different inner shapes with or without surface radiation at relatively higher Rayleigh numbers ($\geq 10^5$) has not been established. As such, the present work addresses the effect of inner shapes, which has pertinent practical applications, on the flow pattern and the heat transfer distribution.

Chapter 2

Formulation

2.1 Model Description

The geometry under consideration is composed of a horizontal annular region between an outer circular cylinder and an inner element with different shapes which are concentrically placed within the outer cylinder as shown in Figure 1.

The outer cylinder and the inner element with different shapes are long enough in the axial direction so that the end effects can be neglected. In our work, both the inner and outer surfaces of the annular region are assumed to be isothermal. This is equivalent to assuming a large thermal conductivity for both the inner and outer surfaces. This isothermal approximation is realistic when the thermal conductivity of both surfaces is at least one order of magnitude higher than that of the air [17].

The inner and outer surfaces are maintained at different constant temperatures. Both walls are assumed to be diffuse gray emitters and reflectors, while the intervening fluid is assumed to be a non-participating medium. All physical properties of the intervening medium are assumed to be constant and evaluated at a reference temperature of $\frac{T_i + T_o}{2}$

except for the density in the buoyancy term which is expressed using the Boussinesq approximation. The reference fluid properties are presented in Table 1. The viscous dissipation and compressibility effects are considered to be negligible.

At higher Ra values, it is important to arrive at a good initial guess and a well-built mesh. We implemented the first of these two requirements by applying a parametric solver which set a prior solution at a lower Ra value as the initial guess for the higher Ra value. The iterative process was tuned for a fast, efficient solution using dimensionless parameters. A well-tuned mesh helps in the convergence of the iterative process. We utilized the triangular free mesh elements in COMSOL. Typically, the free mesh is more robust for natural convection problems because COMSOL automatically refines the mesh at the corners of the domain to capture the boundary layer effects resulting in a faster convergence. In order to find the proper number of elements which would result in a higher accuracy and reasonable computational time, a grid independence test was performed at $T_{ref} = 573K$ and $Ra = 10^6$. The results of this test are given in Table 2. We chose at least 12000 elements for all of our runs based on the results given in Table 2.

2.2 Governing Equations

The choice of a proper characteristic velocity is helpful in non-dimensionalizing the governing equations. For weakly coupled systems, the characteristic velocity is usually based on the free stream velocity. For buoyancy driven flows, we chose a viscous diffusion

velocity $\frac{\sqrt{\beta g \Delta T L}}{\sqrt{Gr}} = \frac{\mu}{\rho L}$ as the characteristic velocity according to Davis [21], where L is

the equivalent annulus gap width. For the elliptical, triangular and square cases, L is the

difference of the radius of the outer cylinder and the radius of the circumscribed circle encompassing the inner shape.

As such the following non-dimensionalized quantities are introduced:

$$x^* = \frac{x}{L}, \quad y^* = \frac{y}{L}, \quad u^* = \frac{uL\rho}{\mu}, \quad v^* = \frac{vL\rho}{\mu}, \quad T^* = \frac{T - T_o}{T_i - T_o}, \quad \text{Pr} = \frac{\mu}{\alpha\rho},$$

$$\text{Ra} = \frac{g\beta(T_i - T_o)L^3\rho}{\alpha\mu}, \quad p^* = \frac{(p + \rho_\infty gy)L^2}{\rho(\mu/\rho)^2}$$

Utilizing the above non-dimensionalized quantities the conservation of mass, momentum and energy equations can be presented as:

$$\frac{\partial u^*}{\partial x^*} + \frac{\partial v^*}{\partial y^*} = 0 \quad (1)$$

$$u^* \frac{\partial u^*}{\partial x^*} + v^* \frac{\partial u^*}{\partial y^*} = -\frac{\partial p^*}{\partial x^*} + \frac{\partial^2 u^*}{\partial x^{*2}} + \frac{\partial^2 u^*}{\partial y^{*2}} \quad (2)$$

$$u^* \frac{\partial v^*}{\partial x^*} + v^* \frac{\partial v^*}{\partial y^*} = -\frac{\partial p^*}{\partial y^*} + \frac{\partial^2 v^*}{\partial x^{*2}} + \frac{\partial^2 v^*}{\partial y^{*2}} + \frac{\text{Ra}}{\text{Pr}} T^* \quad (3)$$

$$u^* \frac{\partial T^*}{\partial x^*} + v^* \frac{\partial T^*}{\partial y^*} = \frac{1}{\text{Pr}} \left(\frac{\partial^2 T^*}{\partial x^{*2}} + \frac{\partial^2 T^*}{\partial y^{*2}} \right) \quad (4)$$

The boundary conditions are expressed as:

$$u^* = v^* = 0 \quad \text{on the inner and outer walls}$$

$$T^* = 1 \quad \text{on the inner wall}$$

$$T^* = 0 \quad \text{on the outer wall}$$

2.3 Radiation Exchange

We increase the Raleigh number by increasing the temperature difference while keeping the other parameters fixed. As such when Ra increases, with the same reference temperature the radiation heat transfer becomes more prominent.

In order to determine the total heat transfer at both the inner and outer walls, we need to take into account both convection and radiation. In the present work, the local Nusselt number is used to include both convection and radiation contributions.

The local Nusselt number is expressed as:

$$Nu = Nu_c + Nu_r = \frac{q_c + q_r}{k(T_i - T_o) / L} \quad (5)$$

where q_c and q_r are local convective and radiative heat fluxes respectively.

The total average Nusselt number which includes the radiation contribution is expressed as:

$$\overline{Nu}_L = \overline{Nu}_c + \overline{Nu}_r = \frac{Q_c + Q_r}{Ak(T_i - T_o) / L} \quad (6)$$

where Q_c and Q_r are the total convective and radiative heat transfer respectively along the surface.

Chapter 3

Validation

Figure 2 (a) shows a comparison of the local equivalent conductivity (Nusselt number) with the results obtained by Kuehn and Goldstein [22]. As can be seen, a very good agreement can be observed. Figure 2 (b) displays a comparison of the dimensionless radial temperature profiles for air at $Ra = 5 \times 10^4$, $Pr=0.7$ with those given in Kuehn and Goldstein [22]. The top vertical position is at zero degree and the bottom curve is at 180 degrees. Once again a very good agreement is observed.

Comparison of the average heat transfer results with those of Kuehn and Goldstein [22] are given in Table 3. As can be seen there is a very good agreement between the current results and those of Kuehn and Goldstein with the average deviation being less than 0.999%.

Comparison of the average heat transfer results of the square inner configuration with those of Chang et al. [23] are given in Table 4. It showed a very good agreement between the current results for a square inner shape and those of Chang et al. (1983) with an average deviation of about 1.043%.

Chapter 4

Results and Discussions

4.1 Streamlines and Isothermals

The streamlines for an annulus made of four nominal inner cross sectional shapes, namely, circle, ellipse, square and a triangle at four different Rayleigh numbers are presented in Figure 3. As it can be seen the flow patterns for all four different inner shapes are somewhat similar. For low Rayleigh numbers, the flow is laminar in the annular region. The fluid near the inner hot surface moves upwards while the fluid near the outer surface moves downwards. This recirculation occurs as the two boundary layers merge creating the so called kidney-shaped core or cellular configuration.

As the Rayleigh number increases, the location of the configuration cell moves up. And when Ra reaches 5×10^5 , the flow begins to show unsteady characteristics which translates into asymmetric and distorted streamlines as can be seen in Figure 3. As the Rayleigh number is increased, the circulation core is further pushed and confined at the top while forming a secondary core. At the same time, the thickness of the both boundary layers diminishes.

The isotherms for these four different inner shapes annuli are given in Figure 4. For $Ra < 5 \times 10^4$, a symmetric pattern is observed for all four inner shapes. As expected, the square and triangular inner shapes show earlier distortion characteristic due to the existence of the corners for these geometries. The elliptical case also shows earlier distortion due to

the larger top space. For higher Rayleigh numbers $Ra > 5 \times 10^4$, the square inner shaped case shows earlier signs of asymmetric characteristics.

Also for higher Rayleigh numbers, heat transfer becomes convective dominated as can be observed by the distorted isotherms and thinner boundary layers. At the same time, thermal stratification can be observed at $Ra = 10^6$. At higher Rayleigh numbers, the thermal boundary layer along the inner cylinder will separate away from the top point and impinges upon the outer cylinder around the top region. The fluid then flows near the outer cylinder towards the bottom displaying the formation of a thermal plume. There also exists a temperature inversion in the region between the two boundary layers.

4.2 Local Nusselt Number

Figures 5 - 8 show a comparison between the local Nusselt number for pure convection and the corresponding one for convection and radiation for $T_{ref} = 573K$ and $1273K$ at $Ra = 10^5$ for four different inner shapes namely cylindrical, elliptical, square and triangular respectively.

For the inner cylindrical annulus case, the inner cylinder boundary layer is quite similar to that near a single horizontal cylinder. The thickness of the boundary layer grows as the fluid flows upward. As such the thinnest boundary layer on the inner cylinder occurs at its bottom, which results in the largest temperature gradient and the highest Nu. The inner

boundary layer impinges on the outer boundary layer establishing the upper plume above the inner cylinder. Figs. 5 (a) and (b) display this behavior.

In Figure 6 (b), it can be seen that the peak value of the local Nusselt number around the outer wall is higher in the elliptical case than the other three inner shape annuli at $T_{ref} = 573K$ and $Ra = 10^5$. In Figure 7 (a), the low values of Nu can be observed between -135 to -45 degrees which corresponds to the bottom plate. In Figure 8 (a), the local Nu is also greatly impacted by the existence of the three corners and the bottom flat surface. Figures 7 (a) and 8 (a) display a wider difference between the radiation added Nu and pure convection around the middle region of the flat surface.

When $T_{ref} = 573K$, as seen in Figs. 5, 6, 7 and 8, the radiation effect on the local heat transfer coefficient is relatively weak especially along the outer wall. However, when $T_{ref} = 1273K$, the local heat transfer becomes radiation dominated as seen in Figs. 5 - 8. Furthermore, for the square and triangular cases, more peaks exist in the radiation modified Nu than that in pure convection as can be seen in Figs. 7 (d) and 8(d). These peaks occur around -180, -90, 0 and 90 degrees respectively for the square inner case, and around -90, 45 and 135 degree for the triangular case.

The radiation corrected Nusselt number distribution at different Rayleigh numbers for the four different inner shapes at $T_{ref} = 573K$ are displayed in Figs. 9 and 10 respectively. As expected, an increase in the Rayleigh number results in larger Nusselt numbers as seen in Figs. 9 and 10.

Comparisons of the radiation and convection local Nusselt number distributions for different inner shape annuli at a given Rayleigh number are displayed in Figure 11. It can be seen that the existence of the corners and the larger top space enhances the heat transfer performance.

As can be seen in Figure 11 (a), the local Nusselt number distribution along the inner surface is the highest for the square case. However, the highest local Nu around the outer surface occurs with the elliptical inner shape annuli as can be seen in Figure 11 (b). As T_{ref} increases to 1273K, it can be seen that the impact of radiation becomes substantially more dominant. Furthermore, it can be seen that for the elliptical, square and triangular inner shape annuli, the local Nusselt number displays a more prominent wavy trend in contrast to the cylindrical inner shape.

4.3 Heat Transfer Correlations

The heat transfer at any point in the domain is represented by the local Nusselt number and the thermal radiation contribution within the annulus is incorporated in the total average Nusselt number, where the total average Nusselt number is defined in Eq. (6).

Using many simulation runs we had established correlations for each of the different inner shape annuli structures in terms of the Rayleigh number dependence and at three pertinent reference temperatures. Since the total average Nusselt number at the inner shape entity is

almost the same [less than 1% difference] as the absolute of that at the outer cylinder, we only present the inner shape average Nusselt number correlations in Table 5.

Chapter 5

Conclusions

An investigation of natural convection in a horizontal concentric annuli with different inner shapes was presented in this work. The effects of different inner shapes on the flow field and heat transfer characteristics were analyzed. Also the effect of surface radiation was incorporated in our investigation. Our model was validated against a number of pertinent results in the open literature.

The existence of the corners in the square and triangular cases and the larger top space in the elliptical annulus was found to enhance the heat transfer performance as compared with that in the cylindrical inner surface case. Radiation was found to play an important role in the overall heat transfer behavior in natural convection at higher temperature levels and higher Rayleigh numbers. We had also established correlations for the total average Nusselt number including the surface radiation.

Table 1. Reference fluid properties

| T_{ref} [K] | P_{ref} [atm] | $\alpha \times 10^6$ [kg/(m·s)] | $\mu \times 10^6$ [kg/(m·s)] | ρ [kg/m ³] | $\beta \times 10^3$ [1/K] |
|------------------|--------------------|------------------------------------|---------------------------------|--------------------------------|------------------------------|
| 293 | 1 | 21.4 | 18.1 | 1.205 | 3.41 |
| 573 | 1 | 71.6 | 29.7 | 0.615 | 1.75 |
| 1273 | 1 | 245.9 | 49.0 | 0.277 | 0.79 |

Table 2. Grid independence test performed at $T_{ref} = 573K$, $Pr = 0.674$ and $Ra = 10^6$

| Number of Elements | Average Nu | Deviation (%) |
|--------------------|------------|---------------|
| 6600 | 7.6151 | 5.2 |
| 8600 | 7.8423 | 2.3 |
| 10000 | 7.9327 | 1.2 |
| 12000 | 7.9957 | 0.4 |
| 17000 | 8.0221 | 0.1 |
| 26000 | 8.0328 | <0.001 |

Table 3. Comparison of the average heat transfer results for a cylindrical annulus with Kuehn and Goldstein [22]

| Ra_L | Pr | L/D_i | Location | K_{eq} | | Deviation % |
|-----------------|-----|---------|----------|--------------|--------------------------|-------------|
| | | | | Present work | Kuehn and Goldstein [22] | |
| 10^2 | 0.7 | 0.8 | Inner | 1.000 | 1.000 | 0 |
| | | | Outer | 1.001 | 1.002 | 0.1 |
| 10^3 | 0.7 | 0.8 | Inner | 1.081 | 1.081 | 0 |
| | | | Outer | 1.082 | 1.084 | 0.18 |
| 3×10^3 | 0.7 | 0.8 | Inner | 1.396 | 1.404 | 0.57 |
| | | | Outer | 1.396 | 1.402 | 0.43 |
| 6×10^3 | 0.7 | 0.8 | Inner | 1.714 | 1.736 | 1.2 |
| | | | Outer | 1.714 | 1.735 | 1.2 |
| 10^4 | 0.7 | 0.8 | Inner | 1.978 | 2.010 | 1.6 |
| | | | Outer | 1.979 | 2.005 | 1.3 |
| 2×10^4 | 0.7 | 0.8 | Inner | 2.374 | 2.405 | 1.3 |
| | | | Outer | 2.375 | 2.394 | 0.8 |
| 3×10^4 | 0.7 | 0.8 | Inner | 2.624 | 2.661 | 1.4 |
| | | | Outer | 2.625 | 2.643 | 0.7 |
| 5×10^4 | 0.7 | 0.8 | Inner | 2.957 | 3.024 | 2.2 |
| | | | Outer | 2.958 | 2.973 | 0.5 |
| 7×10^4 | 0.7 | 0.8 | Inner | 3.191 | 3.308 | 3.5 |
| | | | Outer | 3.193 | 3.226 | 1 |

Table 4. Comparison of the average heat transfer results for a square inner configuration with Chang et al. [23]

| Aspect Ratio | Ra | K_{eq} | | Deviation % |
|--------------|-----------------|--------------|-------------------|-------------|
| | | Present Work | Chang et al. [23] | |
| 0.2 | 10^3 | 1.027 | 1.003 | 2.4 |
| | 5×10^3 | 1.353 | 1.346 | 0.5 |
| | 10^4 | 1.648 | 1.644 | 0.2 |
| | 5×10^4 | 2.452 | 2.457 | 0.2 |
| | 10^5 | 2.837 | 2.846 | 0.3 |
| 0.4 | 10^3 | 1.002 | 1.002 | 0.03 |
| | 5×10^3 | 1.049 | 1.043 | 0.5 |
| | 10^4 | 1.140 | 1.126 | 1.2 |
| | 5×10^4 | 1.687 | 1.617 | 4.3 |
| | 10^5 | 2.007 | 1.991 | 0.8 |

Table 5. Total average Nusselt number correlations at the inner surface for different inner shapes

| Inner shape | Correlation | Conditions | | | Ra Range |
|-------------|---|-------------------|-----------|---|--------------------------|
| Cylindrical | $\overline{Nu}_L = 0.2797Ra_L^{0.2189}$ | $T_{ref} = 293K$ | Pr: 0.703 | $\Delta T = Ra \cdot 9.6356 \times 10^{-9}$ | 1 < Ra < 10 ⁶ |
| | $\overline{Nu}_L = 0.1173Ra_L^{0.3024}$ | $T_{ref} = 573K$ | Pr: 0.674 | $\Delta T = Ra \cdot 2.0233 \times 10^{-7}$ | |
| | $\overline{Nu}_L = 0.0008Ra_L^{0.9884}$ | $T_{ref} = 1273K$ | Pr: 0.719 | $\Delta T = Ra \cdot 5.6569 \times 10^{-6}$ | |
| Square | $\overline{Nu}_L = 0.3203Ra_L^{0.2094}$ | $T_{ref} = 293K$ | Pr: 0.703 | $\Delta T = Ra \cdot 9.6356 \times 10^{-9}$ | |
| | $\overline{Nu}_L = 0.1241Ra_L^{0.3005}$ | $T_{ref} = 573K$ | Pr: 0.674 | $\Delta T = Ra \cdot 2.0233 \times 10^{-7}$ | |
| | $\overline{Nu}_L = 0.0009Ra_L^{0.9881}$ | $T_{ref} = 1273K$ | Pr: 0.719 | $\Delta T = Ra \cdot 5.6569 \times 10^{-6}$ | |
| Triangular | $\overline{Nu}_L = 0.3201Ra_L^{0.2199}$ | $T_{ref} = 293K$ | Pr: 0.703 | $\Delta T = Ra \cdot 9.6356 \times 10^{-9}$ | |
| | $\overline{Nu}_L = 0.1341Ra_L^{0.3036}$ | $T_{ref} = 573K$ | Pr: 0.674 | $\Delta T = Ra \cdot 2.0233 \times 10^{-7}$ | |
| | $\overline{Nu}_L = 0.001Ra_L^{0.984}$ | $T_{ref} = 1273K$ | Pr: 0.719 | $\Delta T = Ra \cdot 5.6569 \times 10^{-6}$ | |
| Elliptical | $\overline{Nu}_L = 0.3221Ra_L^{0.2109}$ | $T_{ref} = 293K$ | Pr: 0.703 | $\Delta T = Ra \cdot 9.6356 \times 10^{-9}$ | |
| | $\overline{Nu}_L = 0.1359Ra_L^{0.2939}$ | $T_{ref} = 573K$ | Pr: 0.674 | $\Delta T = Ra \cdot 2.0233 \times 10^{-7}$ | |
| | $\overline{Nu}_L = 0.0009Ra_L^{0.9831}$ | $T_{ref} = 1273K$ | Pr: 0.719 | $\Delta T = Ra \cdot 5.6569 \times 10^{-6}$ | |

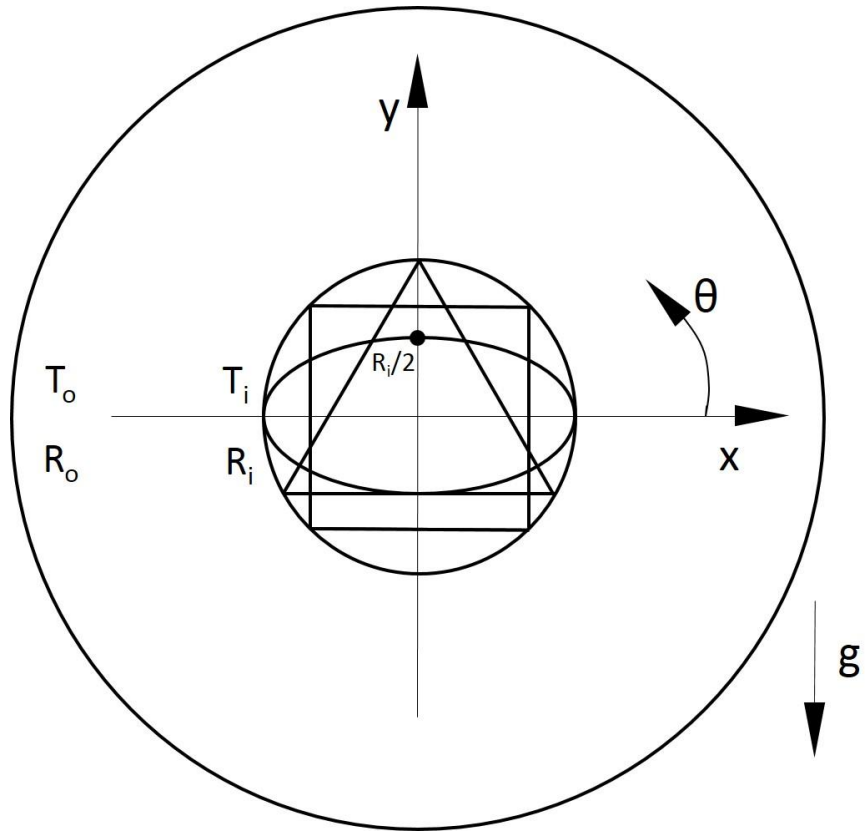
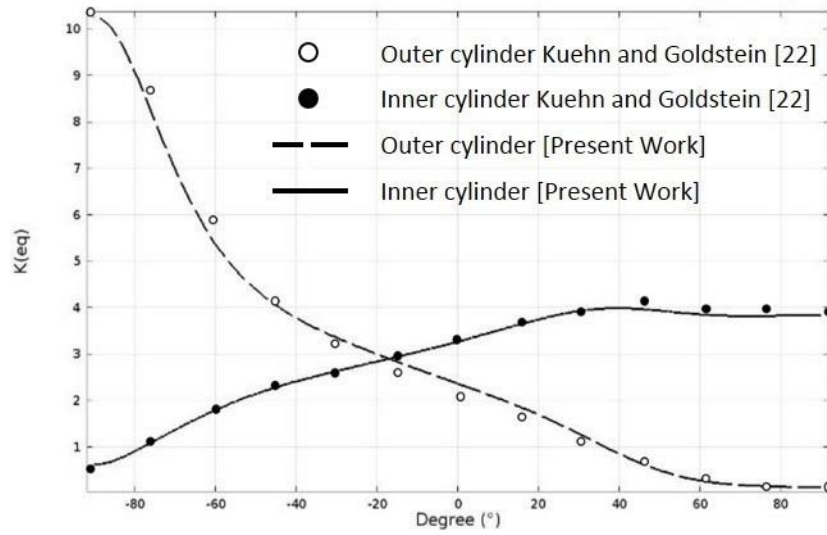
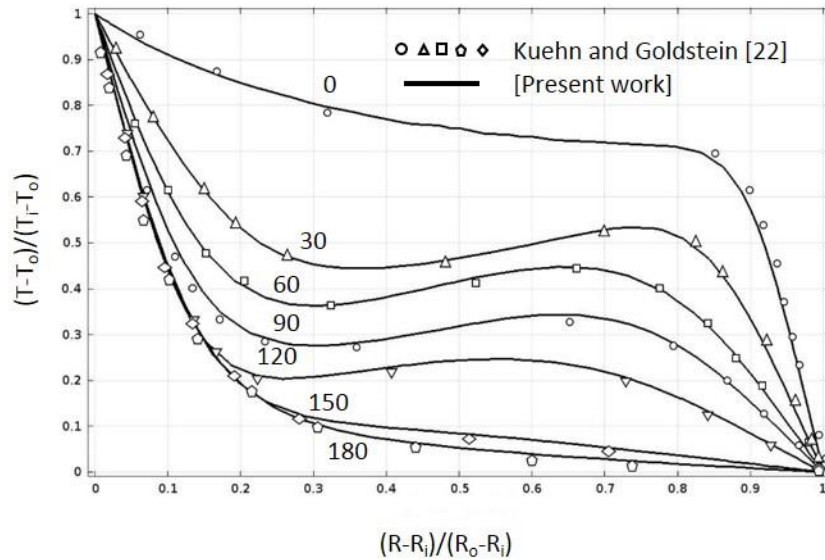


Figure 1. Concentric annuli with different inner shapes



(a) Local equivalent conductivity along the inner and outer surfaces



(b) Dimensionless radial temperature

Figure 2. Comparison of the present results with Kuehn and Goldstein [22] at

$$Ra = 5 \times 10^4$$

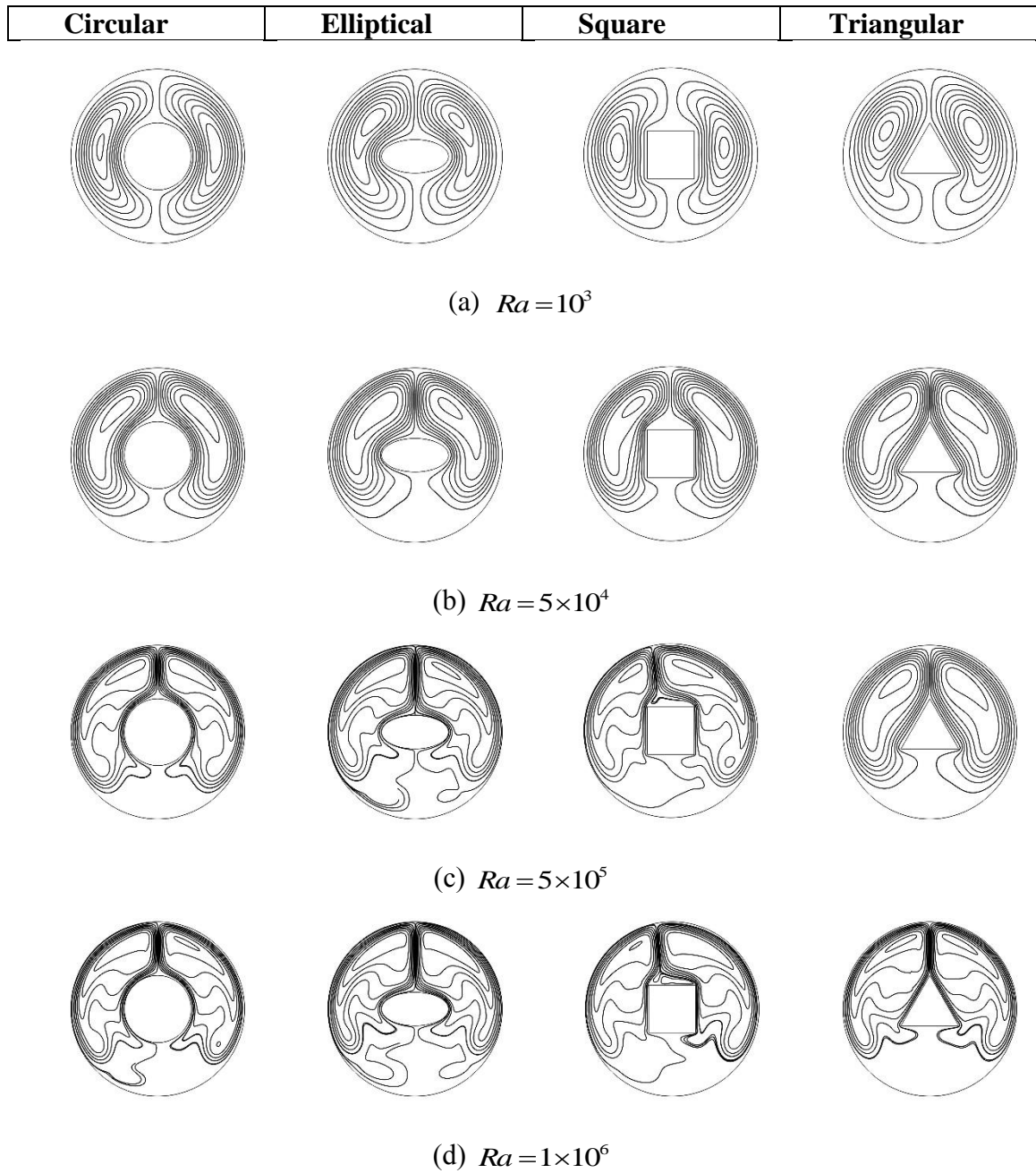


Figure 3. Streamlines in an annulus with different inner shapes: Circular, Elliptical, Square and Triangular at different Rayleigh numbers

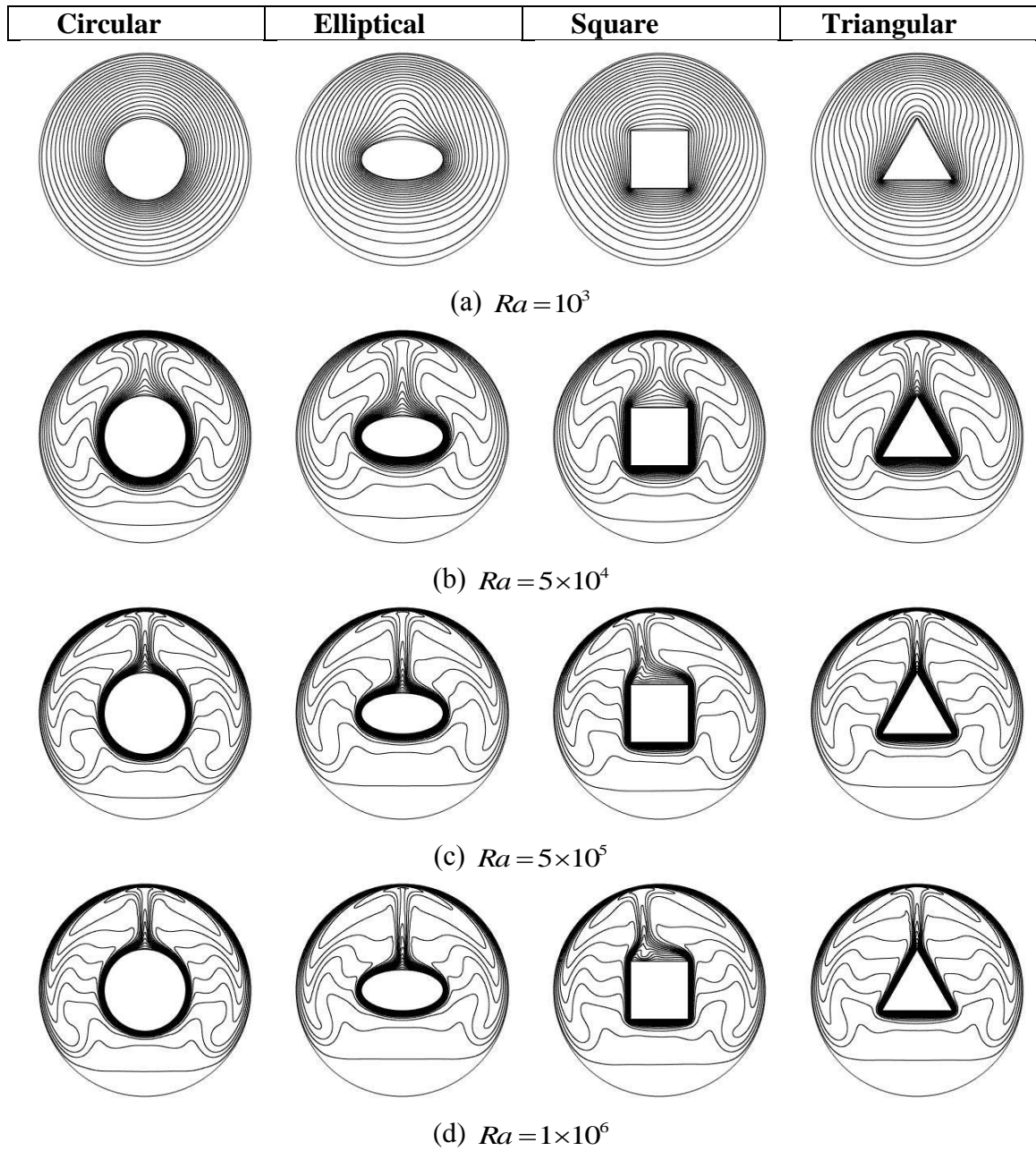
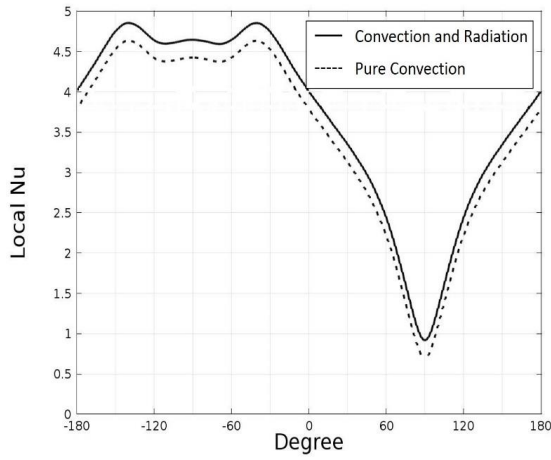
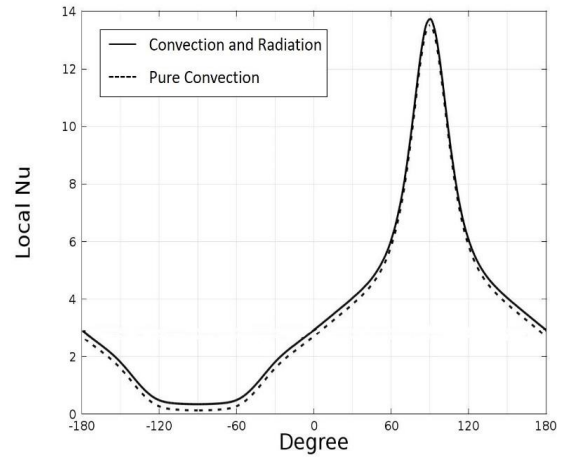


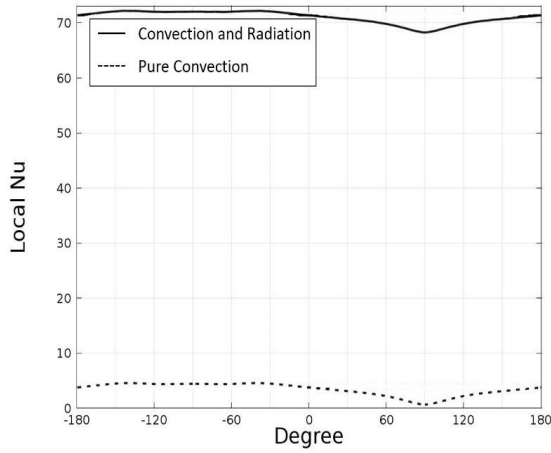
Figure 4. Isotherms in an annulus with different inner shapes:
Circular, Elliptical, Square and Triangular at different Rayleigh numbers



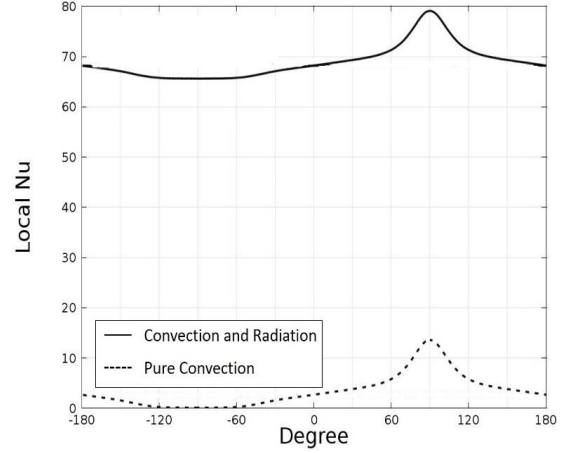
(a) $T_{ref} = 573K$, $Ra = 10^5$ Inner wall



(b) $T_{ref} = 573K$, $Ra = 10^5$ Outer wall

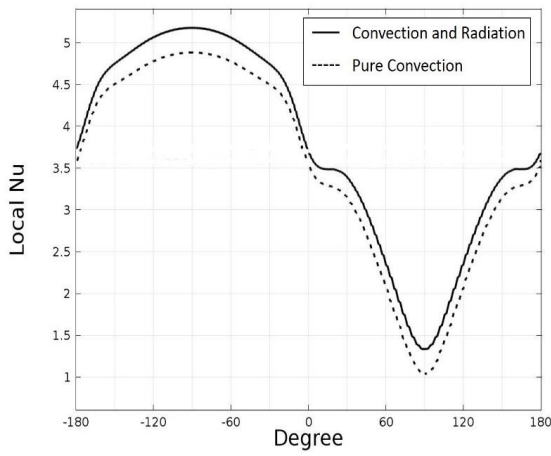


(c) $T_{ref} = 1273K$, $Ra = 10^5$ Inner wall

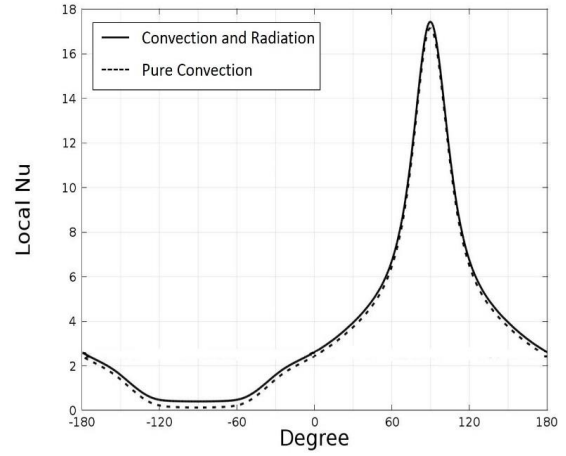


(d) $T_{ref} = 1273K$, $Ra = 10^5$ Outer wall

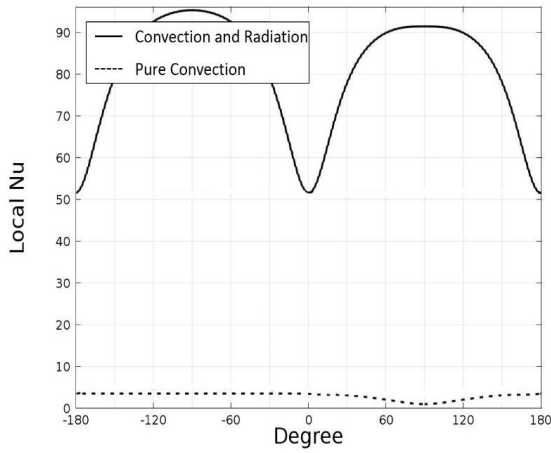
Figure 5. Comparison of the local Nusselt number between pure convection and convection and radiation for a cylindrical annulus



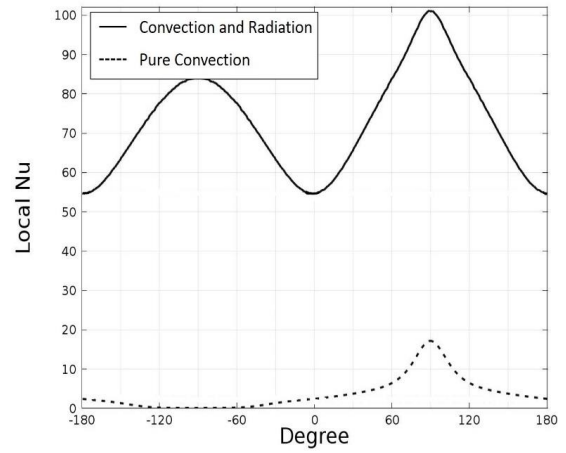
(a) $T_{ref} = 573K$, $Ra = 10^5$ Inner wall



(b) $T_{ref} = 573K$, $Ra = 10^5$ Outer wall

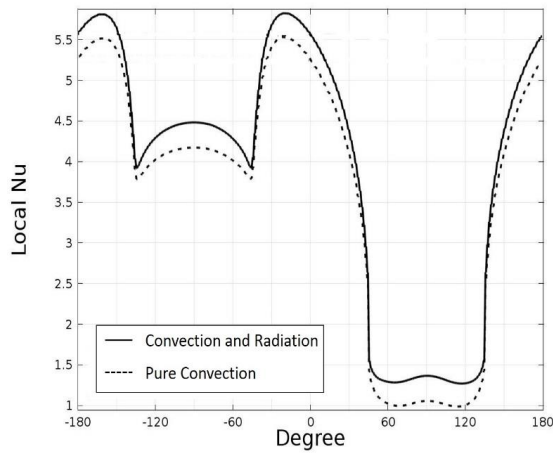


(c) $T_{ref} = 1273K$, $Ra = 10^5$ Inner wall

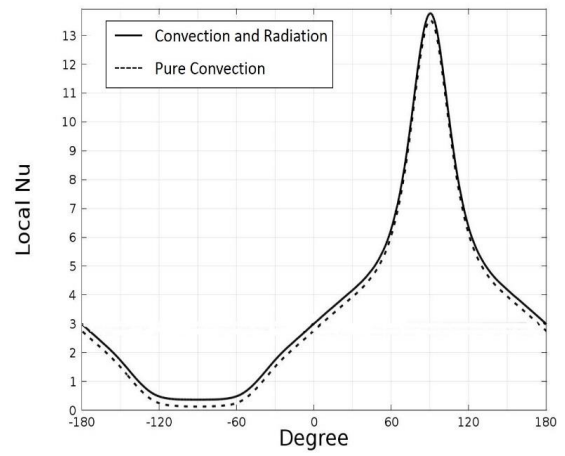


(d) $T_{ref} = 1273K$, $Ra = 10^5$ Outer wall

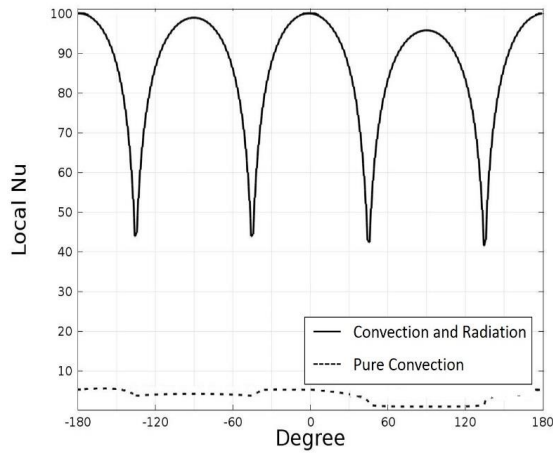
Figure 6. Comparison of the local Nusselt number between pure convection and convection and radiation for an elliptical annulus



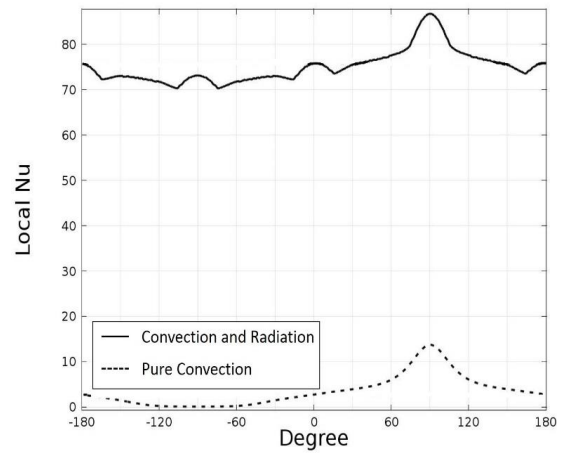
(a) $T_{ref} = 573K$, $Ra = 10^5$ Inner wall



(b) $T_{ref} = 573K$, $Ra = 10^5$ Outer wall



(c) $T_{ref} = 1273K$, $Ra = 10^5$ Inner wall



(d) $T_{ref} = 1273K$, $Ra = 10^5$ Outer wall

Figure 7. Comparison of the local Nusselt number between pure convection and convection and radiation for a square annulus

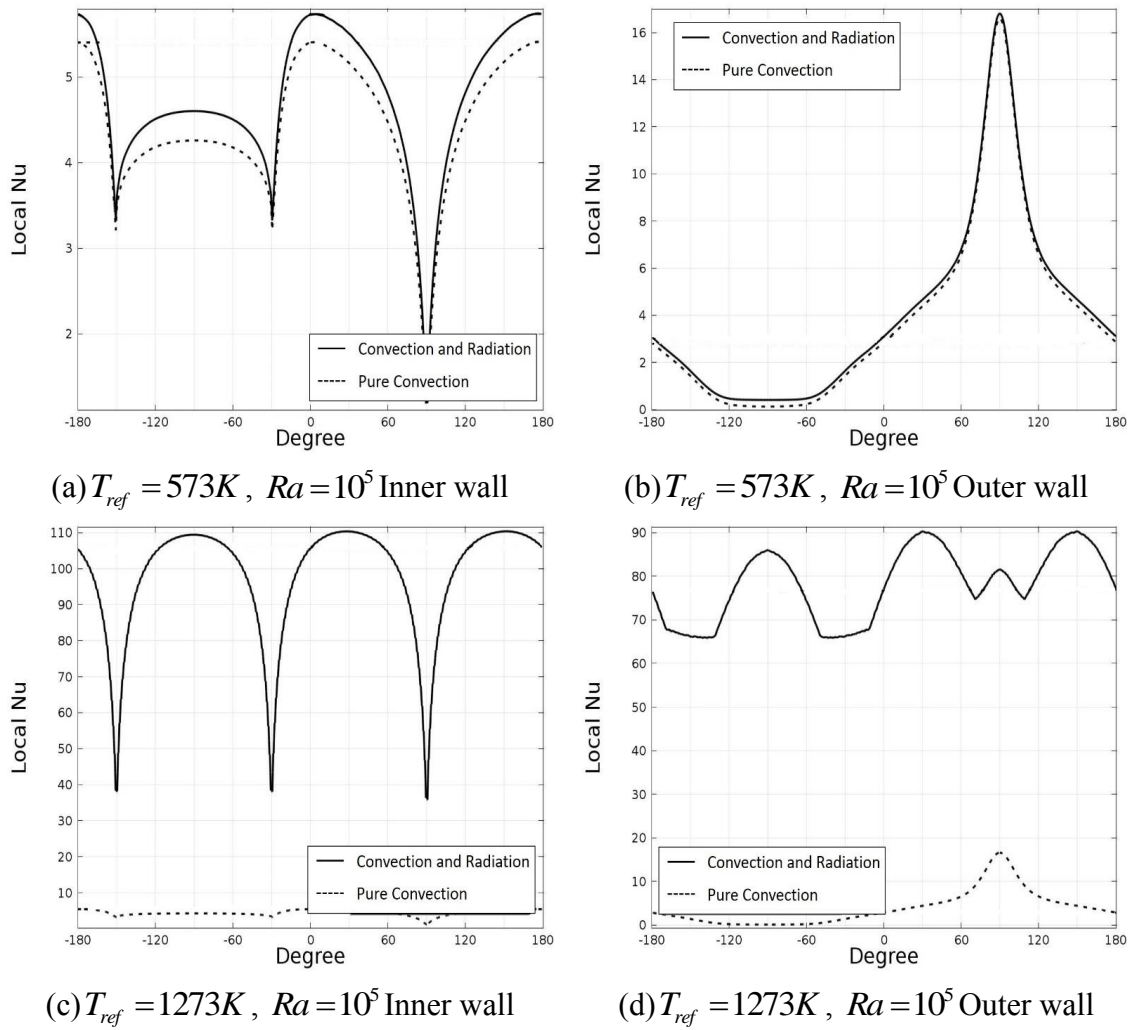
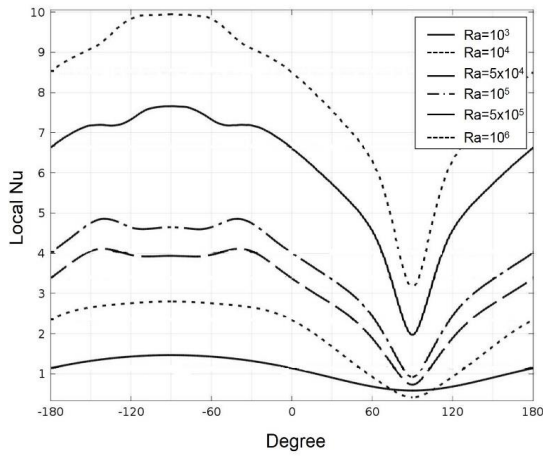
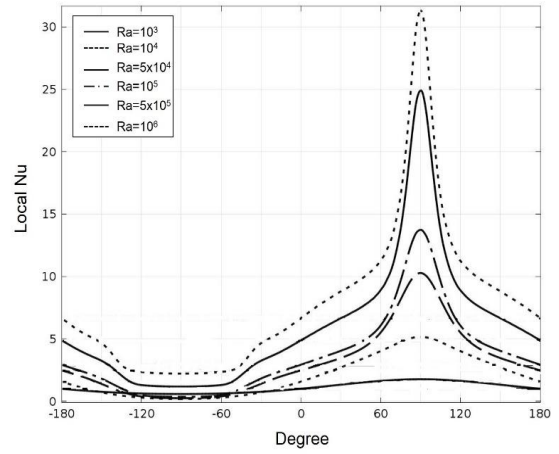


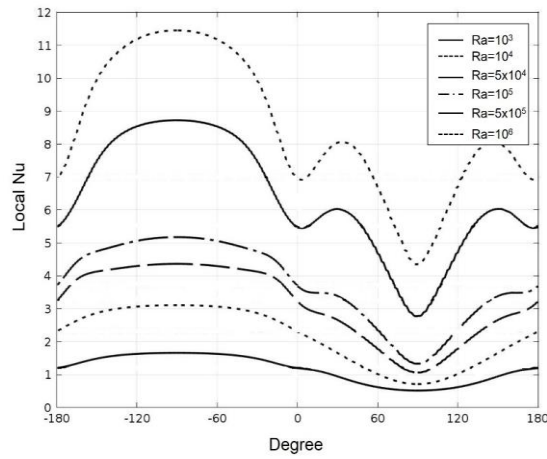
Figure 8. Comparison of the local Nusselt number between pure convection and convection and radiation for a triangular annulus



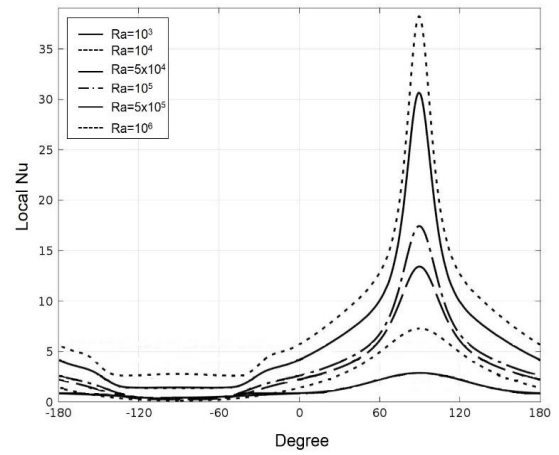
(a) $T_{ref} = 573K$, Inner wall



(b) $T_{ref} = 573K$, Outer wall

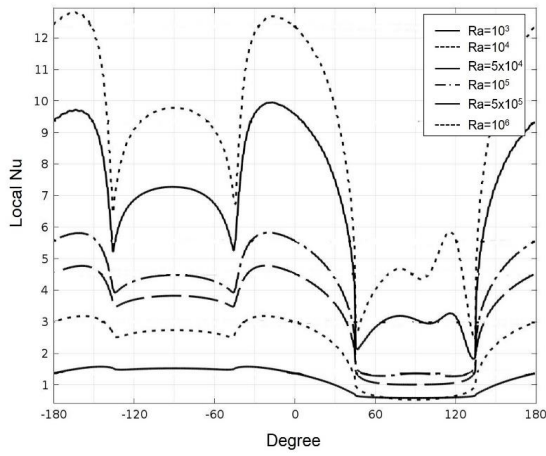


(c) $T_{ref} = 573K$, Inner wall

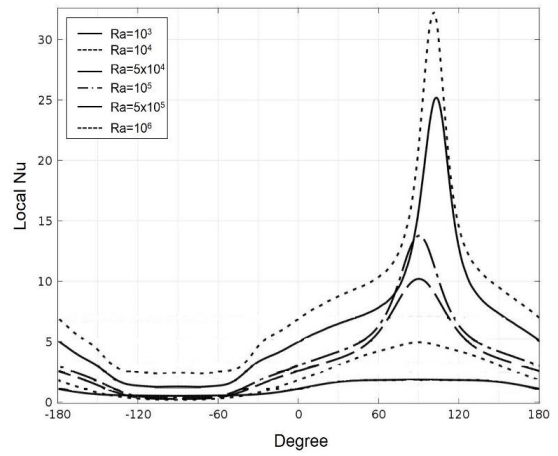


(d) $T_{ref} = 573K$, Outer wall

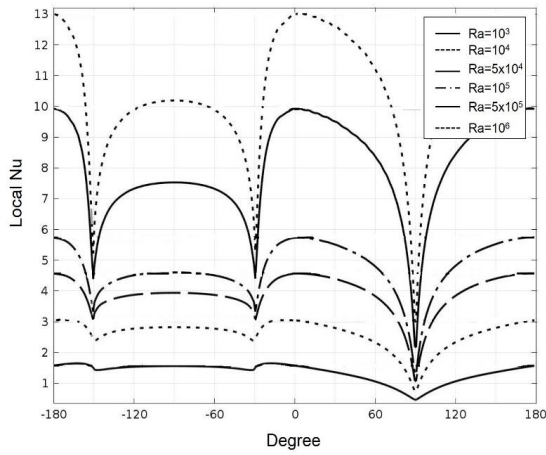
Figure 9. Effect of the Rayleigh number variation on the Nusselt number distribution for
 Cylindrical inner surface (a) Inner wall, (b) Outer wall
 Elliptical inner surface (c) Inner wall, (d) Outer wall



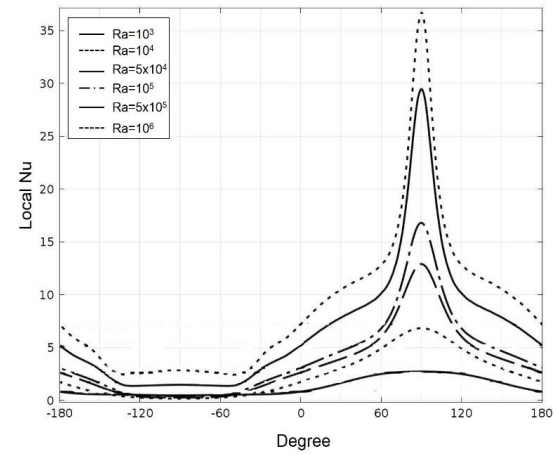
(a) $T_{ref} = 573K$, Inner wall



(b) $T_{ref} = 573K$, Outer wall

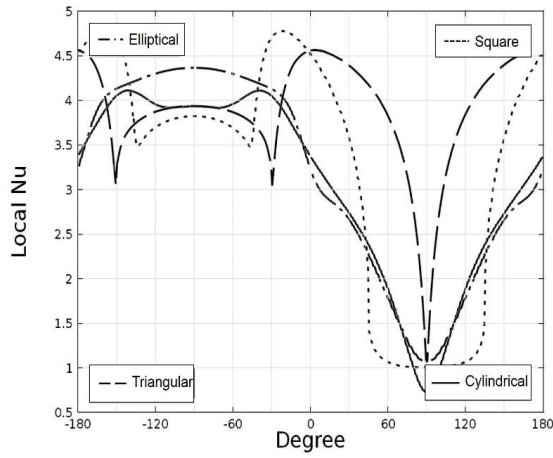


(c) $T_{ref} = 573K$, Inner wall

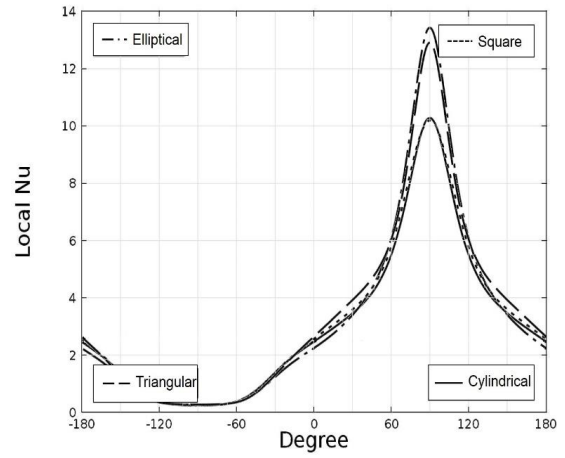


(d) $T_{ref} = 573K$, Outer wall

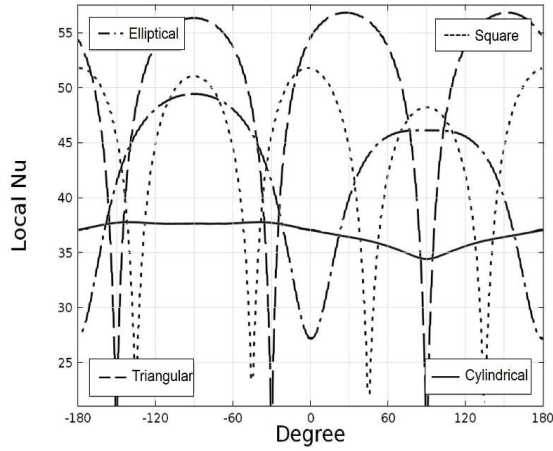
Figure 10. Effect of the Rayleigh number variation on the Nusselt number distribution for
 Square inner surface (a) Inner wall, (b) Outer wall
 Triangular inner surface (c) Inner wall, (d) Outer wall



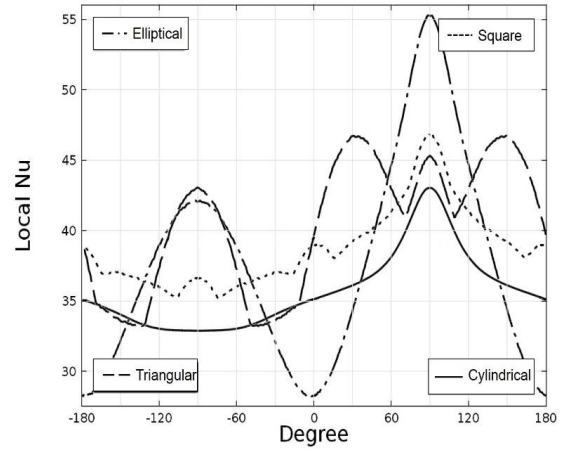
(a) $T_{ref} = 573K$, $Ra = 5 \times 10^4$, Inner wall



(b) $T_{ref} = 573K$, $Ra = 5 \times 10^4$, Outer wall



(c) $T_{ref} = 1273K$, $Ra = 5 \times 10^4$, Inner wall



(d) $T_{ref} = 1273K$, $Ra = 5 \times 10^4$, Outer wall

Figure 11. Comparison of the Nusselt number distribution for different inner shapes at $Ra = 5 \times 10^4$, (a) and (b): $T_{ref} = 573K$ (c) and (d): $T_{ref} = 1273K$

References:

1. D. Angeli, G. S. Barazzi, M. W. Collins and O. M. Kamiyo, A Critical Review of Buoyancy-induced Flow Transitions in Horizontal Annuli, *International Journal of Thermal Sciences*, vol. 49, pp. 2231-2241, 2010.
2. C. J. Ho, Y. H. Lin and T. C. Chen, A Numerical Study of Natural Convection in Concentric and Eccentric Horizontal Cylindrical Annuli with Mixed Boundary Conditions, *International Journal of Heat and Fluid Flow*, vol. 10, pp. 40-47, 1989.
3. C. Shu, Q. Yao, K. S. Yeo and Y. D. Zhu, Numerical Analysis of Flow and Thermal Fields in Arbitrary Eccentric Annulus by Differential Quadrature Method, *Heat and Mass Transfer*, vol. 38, pp. 597-608, 2002.
4. C. Y. Han and S. W. Baek, Natural Convection Phenomena Affected by Radiation in Concentric and Eccentric Horizontal Cylindrical Annuli, *Numerical Heat Transfer Part A: Applications*, vol. 36, pp. 473-488, 1999.
5. A. Shaija and G. S. V. L. Narasimham, Effect of Surface Radiation on Conjugate Natural Convection in a Horizontal Annulus Driven by inner Heat Generating Solid Cylinder, *International Journal of Heat and Mass Transfer*, vol. 52, pp. 5759-5769, 2009.
6. Z. Tan and J. R. Howell, Combined Radiation and Natural Convection in a Two-dimensional Participating Square Medium, *Int. J. Heat Mass Transfer*, vol. 34, pp. 785-793, 1991.
7. M. Akiyama and Q. P. Chong, Numerical Analysis of Natural Convection with Surface Radiation in a Square Enclosure, *Numerical Heat Transfer Part A: Applications: An International Journal of Computation and Methodology*, vol. 31, pp. 419-433, 1997.
8. N. B. Sambamurthy, A. Shaija, G. S. V. L. Narasimham and M. V. K. Murthy, Laminar Conjugate Natural Convection in Horizontal Annuli, *International Journal of Heat and Fluid Flow*, vol. 29, pp. 1347-1359, 2008.
9. X. Xu, G. Sun, Z. Yu, Y. Hu, L. Fan and K. Cen, Numerical Investigation of Laminar Natural Convective Heat Transfer from a Horizontal Triangular Cylinder to its Concentric Cylindrical Enclosure, *International Journal of Heat and Mass Transfer*, vol. 52, pp. 3176-3186, 2009.

10. X. Xu, Z. Yu, Y. Hu, L. Fan and K. Cen, A Numerical Study of Laminar Natural Convective Heat Transfer Around a Horizontal Cylinder Inside a Concentric Air-filled Triangular Enclosure, *International Journal of Heat and Mass Transfer*, vol. 53, pp. 345-355, 2010.
11. Z. Yu, L. Fan, Y. Hu and K. Cen, Prandtl Number Dependence of Laminar Natural Convection Heat Transfer in a Horizontal Cylindrical Enclosure With an Inner Coaxial Triangular Cylinder, *International Journal of Heat and Mass Transfer*, vol. 53, pp. 1333-1340, 2010.
12. R. D. Boyd, Interferometric Study of Natural Convection Heat Transfer in a Horizontal Annulus with Irregular Boundaries, *Nuclear Engineering and Design*, vol. 83, pp. 105-112, 1984.
13. C. Shu, H. Xue and Y. D. Zhu, Numerical Study of Natural Convection in an Eccentric Annulus Between a Square Outer Cylinder and a Circular Inner Cylinder Using DQ Method, *International Journal of Heat and Mass Transfer*, vol. 44, pp. 3321-3333, 2001.
14. F. Moukalled, Natural Convection in the Annulus Between Concentric Horizontal Circular and Square Cylinders, *Journal of Thermophysics and Heat Transfer*, vol. 10, pp. 524-531, 1996.
15. M. Keyhani, F. A. Kulacki and R. N. Christensen, Free Convection in a Vertical Annulus with Constant Heat Flux on the Inner Wall, *Transactions of the ASME*, vol. 105, pp. 454-459, 1983.
16. F. A. W. Hamad, Experimental Study of Natural Convection Heat Transfer in Inclined Cylindrical Annulus, *Solar & Wind Technology*, vol. 6, pp. 573-579, 1989.
17. Y. T. Tsui and B. Tremblay, On Transient Natural Convection Heat Transfer in the Annulus Between Concentric - Horizontal Cylinders with Isothermal Surfaces, *Int. J. Heat Mass Transfer*, vol. 27, pp. 103-111, 1984.
18. K. Vafai and J. Eftefagh, An Investigation of Transient Three-Dimensional Buoyancy-Driven Flow and Heat Transfer in a Closed Horizontal Annulus. *Int. J. Heat Mass Transfer*, vol. 34, pp. 2555-2570, 1991.
19. C. P. Desai and K. Vafai, An Investigation and Comparative Analysis of Two and Three Dimensional Turbulent Natural Convection in a Horizontal Annulus, *Int. J. Heat Mass Transfer*, vol. 37, pp. 2475-2504, 1994.

20. K. Vafai and C. P. Desai, Comparative Analysis of the Finite Element and Finite Difference Methods for Simulation of Buoyancy Induced Flow and Heat Transfer in Closed and Open Ended Annular Cavities, *Numerical Heat Transfer Part A*, vol. 23, pp. 35-59, 1993.
21. G. D. V. Davis, Natural Convection of Air in a Square Cavity: A Bench Mark Numerical Solution, *International Journal for Numerical Methods in Fluids*, vol. 3, pp. 249-264, 1983.
22. T. H. Kuehn and R. J. Goldstein, An Experimental and Theoretical Study of Natural Convection in the Annulus Between Horizontal Concentric Cylinders, *J. Fluid Mech*, vol. 74, pp. 695-719, 1976.
23. K.S. Chang, Y. H. Won and C. H. Cho, Patterns of Natural Convection Around a Square Cylinder Placed Concentrically in a Horizontal Circular Cylinder, *Journal of Heat Transfer*, vol. 105, pp. 273-280, 1983.